Chinese Chemical Letters 37 (2026) 112282

Contents lists available at ScienceDirect

Chinese Chemical Letters

journal homepage: www.elsevier.com/locate/cclet

Concise synthesis and bioactivity evaluation of 5α,6-dihydroveragranine A, (-)-veragranines A & B, and their analogs

Zhi-hao Shang[a], Lei Luo[b,*], Yihao Hu[a], Ren Lai[b,*], Jingjing Wu[a,*]

[a] State Key Laboratory of Synergistic Chem-Bio Synthesis, Frontiers Science Center for Transformative Molecules, Shanghai Key Laboratory for Molecular Engineering of Chiral Drugs, School of Chemistry and Chemical Engineering, Zhangjiang Institute for Advanced Study, Shanghai Jiao Tong University, Shanghai 200240, China

[b] State Key Laboratory of Genetic Evolution and Animal Models, Engineering Laboratory of Peptides of Chinese Academy of Sciences, Key Laboratory of Bioactive Peptides of Yunnan Province, KIZ-CUHK Joint Laboratory of Bioresources and Molecular Research in Common Diseases, National Resource Center for Non-Human Primates, National Research Facility for Phenotypic & Genetic Analysis of Model Animals (Primate Facility), State Key Laboratory of Genetic Evolution & Animal Models, Sino-African Joint Research Center, and New Cornerstone Science Laboratory, Kunming Institute of Zoology, the Chinese Academy of Sciences, Kunming 650201, China

ARTICLE INFO

Article history:
Received 4 November 2025
Revised 11 December 2025
Accepted 12 December 2025
Available online 14 December 2025

Keywords:
Steroidal alkaloids
Biomimetic synthesis
Divergent synthesis
Decarboxylative minisci reaction
Bioactivity evaluation

ABSTRACT

(-)-Veragranines A and B are two steroidal alkaloids that exhibit potent analgesic activity. Herein, we report a 5-step biomimetic synthesis of 5α,6-dihydroveragranine A form hecogenin acetate, which incorporates two well-designed cascade processes that significantly improve the synthetic efficiency. Based on synthesis, an alternative biosynthetic proposal of veragranines was proposed. Subsequently, we developed the first divergent approach enabling the synthesis of veragranines A and B in 10∼12 steps from deoxycholic acid. The synthesis features a photoredox-catalyzed decarboxylative Minisci reaction that achieved good regioselective control and C20 stereochemistry inversion *via* a radical process. Besides, the strategic use of an A/B *cis*-fused starting material enabled late-stage introduction of the $\Delta^{5(6)}$ double bond, simplifying its installation and providing a valuable strategy for the synthesis of related natural products. Notably, we evaluated a series of synthetic intermediates and derivatives of veragranines to assess their *in vitro* analgesic activity. We find that compound **16**, which is easily accessible and features a saturated pyridine as the F-ring, emerges as a promising lead compound.

© 2026 Published by Elsevier B.V. on behalf of Chinese Chemical Society and Institute of Materia Medica, Chinese Academy of Medical Sciences.

Steroidal alkaloids, a class of nitrogen-containing derivatives of natural steroids, constitute a significant group of alkaloids and secondary metabolites present in plants, amphibians, and marine organisms [1,2]. Notably, several steroidal alkaloids have been successfully developed into therapeutic agents, with abiraterone acetate, a steroidal antiandrogen approved by the FDA in 2011 for treating metastatic castration-resistant prostate cancer, being a prominent example [3,4]. This has spurred extensive interest in the synthesis of bioactive steroidal alkaloids with unique structural features, including rearranged skeletons (*e.g.*, cyclopamine [5–8]) and unusual bond connectivities (*e.g.*, batrachotoxin [9–11]) [12].

In light of the global opioid crisis, the development of non-opioid analgesics has become an important topic [13,14]. (-)-Veragranines A (**1**) and B (**2**), two non-opioid steroidal alkaloids isolated from *Veratrum grandiflorum* by Luo and co-workers, have attracted significant attention owing to their potent analgesic activity (Fig. 1a) [15]. These compounds act as $Ca_V2.2$ voltage-gated calcium channel (VGCC) inhibitors, with IC_{50} values of 45.76 ± 1.14 and 7.82 ± 1.10 μmol/L, respectively, making them promising candidates for further biological investigation. However, the extremely low natural abundance of **1** and **2** (approximately 0.00004 wt%) poses a significant challenge for conducting comprehensive biological evaluations. To overcome this limitation, efficient chemical syntheses are not only crucial but also indispensable. Structurally, both **1** and **2** feature a complex 6/6/6/5/6/6 hexacyclic ring system, a unique C12-C23 linkage, and a trisubstituted pyridine ring. Driven by our ongoing interest in the synthesis of steroidal alkaloids [16–19], veragranines have attracted our attention due to their natural scarcity, unique structures, and promising biological activities. Herein, we report our divergent synthesis of **1** and **2** along with their dihydrogenated analog 5α,6-dihydroveragranines A (**3**) through two distinct strategies. Notably, in 2022, concurrent with our study, Shi reported the synthesis of **3** and **4** [20]. During the preparation of this manuscript, Dai disclosed a semisynthesis of **1** and its analogs [21]. It is important to note that our work remains the first approach enabling the synthesis of both **1** and **2**.

* Corresponding authors.
E-mail addresses: luolei@mail.kiz.ac.cn (L. Luo), rlai@mail.kiz.ac.cn (R. Lai), wujingjingsjtu@sjtu.edu.cn (J. Wu).

https://doi.org/10.1016/j.cclet.2025.112282
1001-8417/© 2026 Published by Elsevier B.V. on behalf of Chinese Chemical Society and Institute of Materia Medica, Chinese Academy of Medical Sciences.

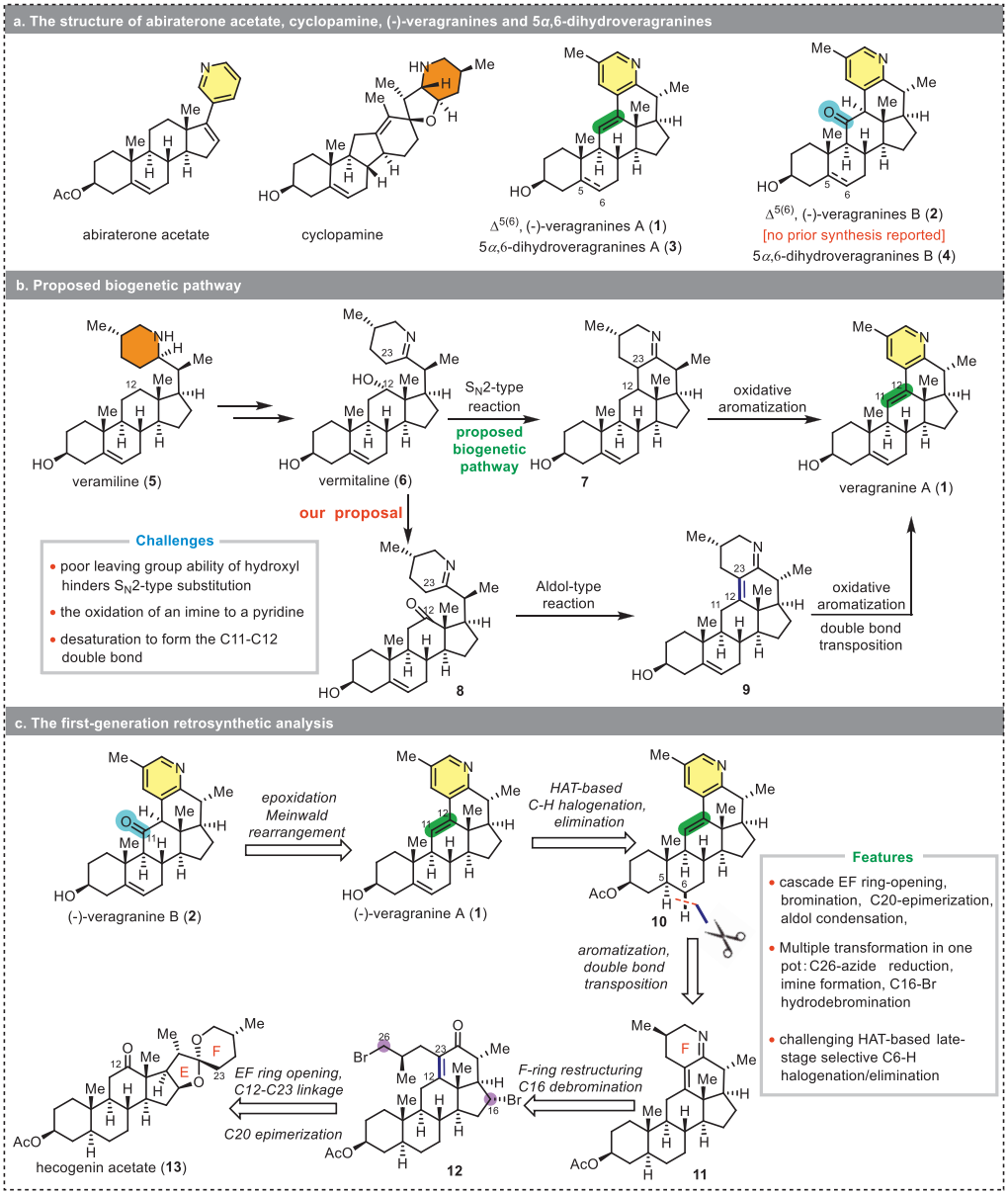


Fig. 1. Proposed biosynthesis pathways and the first-generation retrosynthetic analysis. (a) The structure of abiraterone acetate, cyclopamine, (-)-veragranines and 5α,6-dihydroveragranines. (b) Proposed biogenetic pathway. (c) The first-generation retrosynthetic analysis.

Two similar biosynthetic pathways were proposed by Luo and Dai [15,21], where they believed **1** and **2** could be biosynthesized from veramiline (**5**), a major steroidal alkaloid of *V. grandiflorum*. According to their hypothesis, veramiline could be converted to vermitaline (**6**) *via* an enzymatic C12-H hydroxylation and dehydrogenation of the piperidine ring. Subsequently, Luo postulated a stepwise process: Initially, oxidative aromatization of the F ring to a pyridine, followed by an S_N2-type substitution to form the C23-C12 σ-bond. Whereas Dai proposed an alternative sequence, first, construction of the C23-C12 σ-bond through a similar S_N2 reaction, then oxidative aromatization and epimerization of the C20 stereochemistry to give **1**. We conducted a comprehensive evaluation of the biomimetic approach as a potential synthetic pathway. Based on a detailed analysis, we concluded that the S_N2-type substitution could be challenging because the hydroxyl group is a poor leaving group. Additionally, there could be difficulties in the subsequent steps, including the oxidation of an imine to a pyridine and the desaturation to form a C11-C12 double bond. We then proposed an alternative biosynthetic pathway involving two key transformations: First, the selective oxidation of the C12-OH in **6** to yield ketone **8**; second, an aldol condensation to form the C23-C12 bond, generating the α,β-unsaturated imine **9**, which subsequently undergoes oxidative aromatization followed by double bond transposition to afford **1** (Fig. 1b).

Based on our biosynthetic proposal, the first-generation retrosynthetic analysis is presented in Fig. 1c. Since the C11 ketone of **2** could be constructed from a C11-C12 epoxide *via* Meinwald rearrangement [20], we prioritized the synthesis of **1**. The $\Delta^{5(6)}$ double bond of **1** could be introduced from **10**, through a challenging HAT-based late-stage C6-H halogenation/elimination strategy. We envisaged **10** could be obtained from **11** through our proposed biomimetic oxidative aromatization, double bond transposition. Then **11** could be synthesized from **12** through C26 azidination followed by reductive imine formation and C16 debromination. Moreover, **12** could be easily prepared from hecogenin acetate (**13**) through $BF_3{\cdot}Et_2O$-promoted bromination/ring-opening of

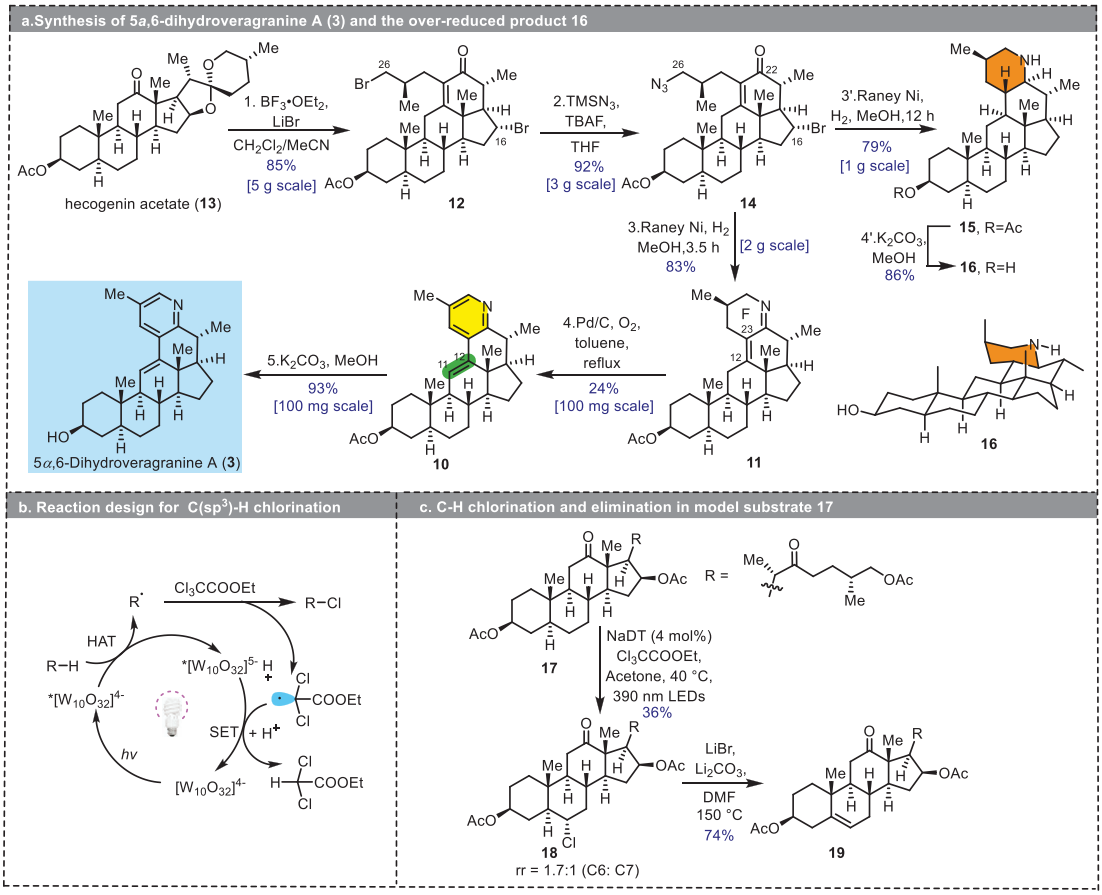


Fig. 2. Synthesis of 5α,6-dihydroveragranine A (**3**), the over-reduced product **16**, and the development of a HAT-based C(sp^3)-H chlorination.

steroidal sapogenins, the methodology we previously developed [16].

As shown in Fig. 2a, our synthesis started with the preparation of dibromide compound **12** from **13**. Then regioselective azidination of the less hindered C26-Br gave the desired product **14** in 92% yield. We hypothesized that the C26-azide reduction, C22 imine formation, and C16-Br hydrodebromination transformations could be performed in the same flask. After systematic optimization (see Supporting Information for details), we discovered that the Raney Ni/H_2 reduction conditions facilitated this cascade transformation efficiently, affording the desired product **11** in 83% yield. Remarkably, extending the reaction time enabled the formation of the complete hydrogenation product **15** in high yield. Subsequent hydrolysis afforded product **16**, featuring a piperidine as the F ring, which was also evaluated for bioactivity. With **11** in hand, we proceeded to investigate the key biomimetic oxidative aromatization of the F ring with transposition of the $\Delta^{12(23)}$ double bond to $\Delta^{11(12)}$. After unsuccessful attempts with reagents such as DDQ, IBX, and others, we found that using Pd/C as the catalyst and oxygen as the oxidant provided the desired product **10** in 24% yield. After hydrolysis, the desired product 5α,6-dihydroveragranine A (**3**) was obtained in good yield.

In order to obtain the natural product veragranine A (**1**), we decided to implement a strategy featuring HAT-based late-stage C(sp^3)-H halogenation/elimination [22–28]. Inspired by the pioneering work reported by Wu [29], we designed a decatungstate photoredox-catalyzed C–H chlorination (Fig. 2b). Prior to applying the desired substrate **10**, we selected an easily accessible compound **17** as the model substrate. After optimization (see Supporting Information for details), the desired C–H chlorination product could be obtained in 36% yield, with 1.7:1 (C6:C7) regioselectivity (Fig. 2c). A further elimination step was carried out to transfer the C6-Cl product **18** into $\Delta^{5(6)}$ compound **19**. Although this strategy could be successfully applied to introduce a $\Delta^{5(6)}$ double bond in model substrate **17**, unfortunately, it did not work on real substrate **10**. After spending half a year studying HAT-based C–H functionalization conditions to introduce the $\Delta^{5(6)}$ double bond, we could not find an efficient solution. We therefore started our second-generation synthetic route.

Given the challenge of late-stage introduction of a $\Delta^{5(6)}$ double bond in the A/B *trans*-fused steroid system, and considering that it is easier to introduce a $\Delta^{4(5)}$ double bond in A/B *cis*-fused steroids (which can further undergo transposition to $\Delta^{5(6)}$) [30,31], we chose the abundantly available deoxycholic acid (**24**) as the starting material. Our second-generation retrosynthetic analysis is presented in Fig. 3, where both **1** and **2** could be synthesized from **20** through late-stage oxidation to introduce a $\Delta^{4(5)}$ double bond. According to Shi's result [20], late-stage introduction of a C11 ketone group in **2** from the $\Delta^{11(12)}$ olefin in **20** is also feasible. The E ring of **20** could be constructed through a photoredox-catalyzed decarboxylative Minisci reaction from **21** [32–34]. The pyridine fragment of **21** could be introduced through the addition of organolithium reagent **22** to the C12-ketone of **23**. Subsequent elimination of the newly formed C12-OH afforded the $\Delta^{11(12)}$ double bond. Also, the C22 carboxylic acid of **21** could be easily obtained *via* oxidative cleavage of the terminal $\Delta^{22(23)}$ olefin of **23**. In turn, **23** could be constructed from **24** through photoredox-catalyzed oxidative degradation of the side chain [35,36].

As the key step in our synthetic plan, the decarboxylative Minisci reaction faced two major challenges. First, radical cycliza-

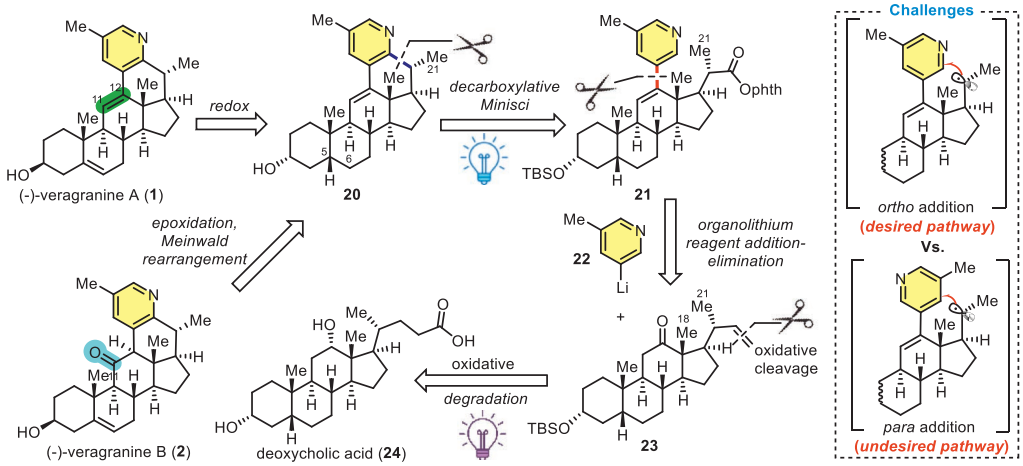


Fig. 3. The second-generation retrosynthetic analysis.

tion to the pyridine ring could lead to *ortho*-addition (C22) and *para*-addition (C24), thus regioselectivity needs to be controlled. We believed that the Me- group on the pyridine ring (C25) would make the *para*-addition to the C24 position more sterically hindered, therefore our desired *ortho*-addition product would be the major product. Second, the C21-Me configuration needs to be inverted through this step. Since the decarboxylation step would generate a radical at the C20, we hypothesized that during the cyclization, the C21-Me would prefer to be in the pseudo-equatorial position to avoid strong 1,3-diaxial interaction with the C18-Me, thus providing the desired inverted stereochemistry at C20.

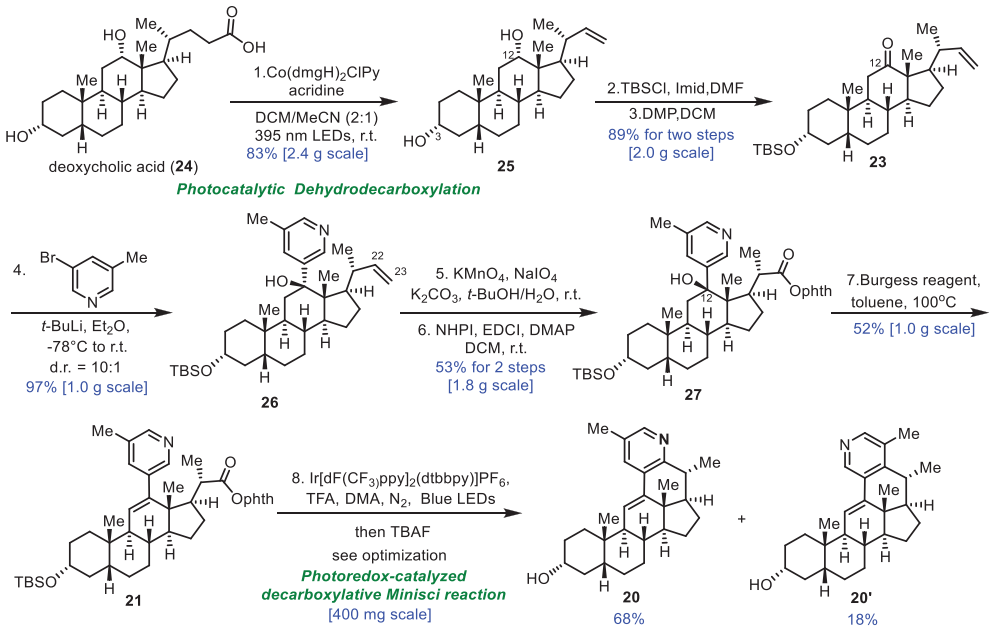
As illustrated in Fig. 4, utilizing the method developed by the Ritter and Larionov group [35,36], we initiated our synthesis with photoredox-catalyzed decarboxyolefination of **24**, yielding the desired product **25** in 83 % yield. After selective TBS-protection of the less hindered C3-OH and subsequent Dess-Martin oxidation of the C12-OH, intermediate **23** was obtained in 89 % yield on a 2-gram scale. Following successful preparation of organolithium reagent **22** through *in-situ* lithium-bromine exchange, we investigated the addition of the **22** to the C12-ketone of **23**.

To our delight, this reaction proceeded smoothly, affording the desired product **26** in 97 % yield, with a 10:1 diastereomeric ratio. We next explored the oxidative cleavage of the terminal $\Delta^{22(23)}$ olefin to a carboxylic acid. Several conventional methods, including the $RuCl_3/NaIO_4$ system or ozonolysis followed by Pinnick oxidation, gave low yields (see Supporting information for details). Fortunately, we found that with a basic $KMnO_4/NaIO_4$ system [37], the desired product could be obtained in moderate yield. Since the desired carboxylic acid was highly polar and difficult to isolate, the crude product was directly subjected to the EDCI condensation. Delightfully, the desired redox-active-ester **27** could be obtained in 53 % yield. We then proceeded to perform a C12-OH elimination reaction to introduce the $\Delta^{11(12)}$ double bond. Delightfully, with Burgess reagent, the desired product **21** was obtained in 52 % yield. Other elimination conditions, such as $SOCl_2$/pyridine and $POCl_3$/pyridine, were found to be unsuccessful (see Supporting information for details).

We then proceeded to investigate the key decarboxylative Minisci reaction. Initially, the photoredox-catalyzed direct oxidative decarboxylative Minisci reaction from the carboxylic acid was also tested [38–40], but it failed to yield the desired product. Consequently, we shifted to redox-active-ester **21**. As shown in Fig. 4, after screening a series of conditions, the desired product **20** was successfully synthesized in 68 % yield, accompanied by 18 % of the regioisomer **20′**, using $Ir[dF(CF_3)ppy]_2(dtbbpy)PF_6$ as the photocatalyst, TFA (1.5 equiv.) as the acid, and DMA as the solvent under blue LED irradiation (Entry 1). Using $Ir(ppy)_3$ as the photocatalyst resulted in a lower yield of **20** and reduced regioselectivity, whereas photocatalysts $Ru(bpy)_3Cl_2$ and Eosin Y showed no reactivity (entries 2–4). Both reducing or increasing the amount of TFA resulted in lower yields (entries 5 and 6). Replacement of TFA with TsOH or H_2SO_4 also decreased the yield (entries 7 and 8). Switching the solvent to DMF resulted in a decrease in the yield and regioselectivity, whereas MeCN provided a comparable yield and improved regioselectivity (entries 9 and 10).

With the advanced intermediate **20** in hand, we proceeded to finish the divergent synthesis of **1** and **2** (Fig. 5). After IBX/NMO oxidation [41], **20** was converted to $\Delta^{4(5)}$-3-one product **28** in 54 % yield. Then, after enolization with *t*-BuOK/*t*-BuOH and subsequent quenching in acidic conditions, the $\Delta^{4(5)}$ double bond underwent transposition to $\Delta^{5(6)}$ [30]. Finally, reduction of the C3-ketone with $NaBH_4$ afforded the desired natural product (-)-veragranine A (**1**) in 83 % yield. Next, we focused on the synthesis of **2**. Treatment of **20** with NBS/HOAc in aqueous THF solution, followed by hydrolysis of the crude bromohydrin acetate afforded β-epoxide **29** in 68 % yield. Subsequent IBX/NMO oxidation yielded $\Delta^{4(5)}$-3-one product **30** in 54 % yield. The Et_2AlCl-promoted Meinwald rearrangement afforded the C11-ketone product **31** in 82 % yield [20]. Subsequently, after a similar $\Delta^{4(5)}$ double bond transposition to $\Delta^{5(6)}$ and selective reduction of the less hindered C3-ketone with $NaBH_4$, the desired natural product (-)-veragranine B (**2**) was obtained in 64 % yield.

Prior to initiating our biological assays, we noted that Dai *et al.* had concurrently reported their synthesis of veragranine A and analogs [21]. To secure the novelty of our research and facilitate early-stage scholarly communication, we therefore made our synthetic routes to veragranines A and B publicly available as a preprint on ChemRxiv [42]. Subsequently, with (-)-veragranines A/B, 5α,6-dihydroveragranine A and their analogs in hand (Fig. 6, top), we performed a comprehensive evaluation of their bioactivity to explore their therapeutic potential. The detailed synthetic procedures for analogs **32–35** are provided in Supporting information. Building on prior reports demonstrating that veragranines A and B potently inhibit $Ca_V2.2$ channels [15], key mediators of nociceptive signaling, we employed whole-cell patch-clamp recordings to evaluate the inhibitory effects of a panel of synthetic derivatives. Initial screening revealed compound **16** as the most potent inhibitor, exhibiting activity comparable to the natural compound veragranine B (Figs. 6A and B). Concentration-response analysis revealed that **16** suppressed $Ca_V2.2$ currents in a concentration-dependent man-



Entry[a]	Variation	Results[b]	Entry[a]	Variation	Results[b]
1	none	**20** (68%); **20'** (18%)	6	TFA (2.0 equiv.)	**20** (43%); **20'** (9%)
2	$Ir(ppy)_3$ as photocatalyst	**20** (47%); **20'** (24%)	7	TsOH (1.5 equiv.) as acid	**20** (44%); **20'** (13%)
3	$Ru(bpy)_3Cl_2$ as photocatalyst	**20** (trace); **20'** (trace)	8	H_2SO_4 (1.5 equiv.) as acid	**20** (47%); **20'** (13%)
4	Eosin Y as photocatalyst	**20** (trace); **20'** (trace)	9	DMF as solvent	**20** (39%); **20'** (24%)
5	TFA (1.2 equiv.)	**20** (54%); **20'** (15%)	10	MeCN as solvent	**20** (66%); **20'** (5%)

[a]Standard conditions: **21** (0.15 mmol), Ir[dF(CF3)ppy]2(dtbbpy)]PF6 (2 mol%), TFA (1.5 equiv.), DMA (0.1 M), N2, Blue LEDs, then TBAF(1.5 equiv.). [b]Isolated yields.

Fig. 4. Optimization of the decarboxylative Minisci reaction enabled the synthesis of intermediate **20**.

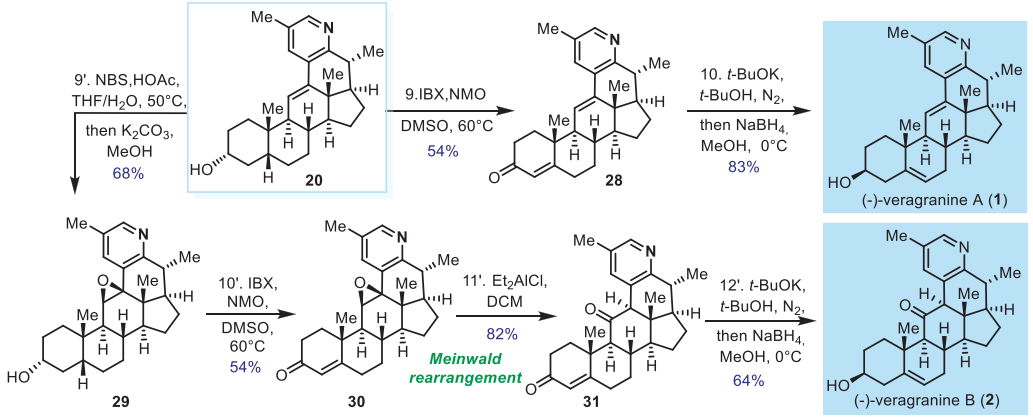


Fig. 5. Divergent synthesis of (-)-veragranines A and B.

ner (Fig. 6C), with a half-maximal inhibitory concentration (IC_{50}) of 15.96 ± 1.71 μmol/L at a holding potential of −80 mV (Fig. 6D). Notably, the IC_{50} of **16** was intermediate between those of veragranines A and B, positioning it as a synthetic analog with balanced efficacy (Figs. 6D and E).

Steady-state current-voltage (*I-V*) relationship studies further demonstrated that **16** did not alter the voltage sensitivity of $Ca_V2.2$ channels, as indicated by the unperturbed activation curve (Figs. 6F-H). This behavior mirrored the effects of **16** and veragranines, indicating a shared mechanistic basis involving direct interaction with the channel pore region to block ion permeation, rather than modulation of voltage-gated domains. Combining high synthetic efficiency, a streamlined preparation route, and selective $Ca_V2.2$ antagonism, **16** emerges as a promising lead compound for the development of targeted therapeutics against $Ca_V2.2$-dependent pathologies.

In conclusion, we have explored two distinct strategies for the synthesis of veragranines. The first approach enabled the concise synthesis of 5α,6-dihydroveragranine A in 5 steps (14.5% overall yield) from hecogenin acetate, featuring: (1) Two well-designed cascade processes that significantly improve the synthetic efficiency; (2) Differing from the proposed S_N2-type biogenetic pathway, we proposed an aldol-type condensation to form the α,β-unsaturated imine, which was successfully converted into veragra-

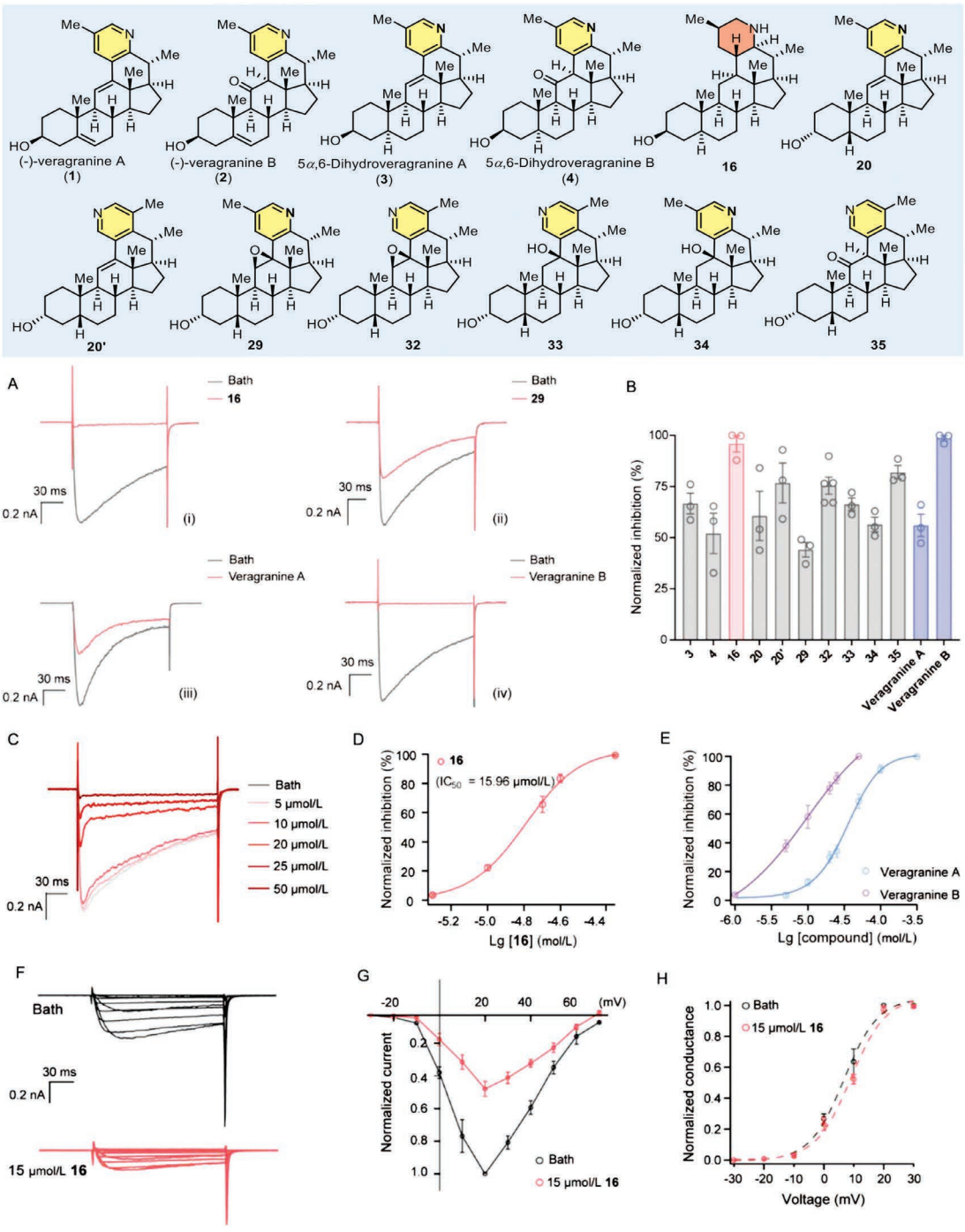


Fig. 6. Bioactivity evaluation of veragranine analogs on the electrophysiological properties of human $Ca_V2.2$ channel. (A) Representative current traces of $Ca_V2.2$ channels under bath (control), **16** (50 μmol/L), **29** (50 μmol/L), veragranine A (50 μmol/L) and veragranine B (50 μmol/L), treatments (scale: 30 ms, 0.2 nA). (B) Normalized inhibition percentages of synthetic derivatives, veragranines A and B acting on $Ca_V2.2$ channels. Compound **16** exhibits the strongest inhibition, comparable to veragranine B. Concentration, 50 μmol/L. (C) Representative whole-cell $Ca_V2.2$ currents elicited by a 150 ms depolarization of +10 mV in the absence and presence of different concentrations of **16**. (D) Dose-response curves displaying the **16**-induced inhibition of the $Ca_V2.2$ channel. Data were fit using a Hill equation. The IC_{50} and slope factor values are 15.96 ± 1.71 μmol/L and 1.85 ± 0.59 ($n = 6$ cells). (E) Concentration-dependent inhibition of $Ca_V2.2$ currents by veragranines A and B. The IC_{50} of veragranine A and veragranine B are 7.99 ± 1.03 and 34.56 ± 1.95 μmol/L, respectively. (F) Representative $Ca_V2.2$ current traces in response to various membrane potentials from −80 mV to +70 mV in 10 mV increments before (black) and after (red) application of 15 μmol/L compound **16**. (G) Current-voltage (*I-V*) relationship for $Ca_V2.2$ currents before and after application of 15 μmol/L compound **16** ($n = 3$). (H) Normalized conductance (G/G_{max}) *versus* voltage relationships for the traces as in G. Data were fit using the Boltzmann equation ($n = 3$).

nines through oxidative aromatization and double bond transposition, thereby supporting this alternative biosynthetic route. The second strategy provided the first divergent synthesis of veragranines A and B in 10–12 steps (6%–2.6% overall yield) from deoxycholic acid, featuring: (1) Photoredox-catalyzed decarboxylative Minisci reaction for E ring closure with C20 stereoinversion; (2) Late-stage introduction of the $\Delta^{5(6)}$ double bond *via* a strategic A/B *cis*-fused intermediate, circumventing regioselectivity challenges between the $\Delta^{11(12)}$ and $\Delta^{5(6)}$ double bonds and enabling the first synthesis of (−)-veragranine B. After further bioactivity studies of veragranines and their 10 analogs, we are delighted to identify the easily accessible compound **16** as a promising lead

compound. Its dual advantages of mechanistic clarity and synthetic feasibility establish it as a versatile scaffold for probing $Ca_V2.2$ biology and accelerating analgesic drug discovery.

CRediT authorship contribution statement

Zhi-hao Shang: Methodology, Investigation, Data curation. **Lei Luo:** Writing – original draft, Investigation, Data curation. **Yihao Hu:** Investigation. **Ren Lai:** Supervision. **Jingjing Wu:** Writing – review & editing, Supervision, Project administration, Funding acquisition.

Declaration of competing interest

The authors declare that they have no known competing financial interests or personal relationships that could have appeared to influence the work reported in this paper.

Acknowledgments

The authors gratefully acknowledge Prof. Jinghan Gui from Shanghai Institute of Organic Chemistry (SIOC) and Prof. Phillip. S. Grant from Nanyang Technological University for helpful discussion. We thank Prof. Yong Shi from Yunnan University for providing 5α,6-dihydroveragranine B for bioactivity study. Financial support was provided by National Natural Science Foundation of China (NSFC, Nos. 22101173 and 32522015), Fundamental Research Funds for the Central Universities (No. 24X010301678), "Thousand Talents Plan, Youth Project", and Yunnan Major Science and Technology Project (No. 202402AA310010).

Supplementary materials

Supplementary material associated with this article can be found, in the online version, at doi:10.1016/j.cclet.2025.112282.

References

[1] M.L. Xiang, B.Y. Hu, Z.H. Qi, et al., Nat. Prod. Bioprospect. 12 (2022) 23.
[2] Q.W. Jiang, M.W. Chen, K.J. Cheng, et al., Med. Res. Rev. 36 (2016) 119–143.
[3] H.B. Schultz, T.R. Meola, N. Thomas, C.A. Prestidge, Int. J. Pharm. 577 (2020) 119069.
[4] J. Cassinello, T. Domínguez-Lubillo, M. Gómez-Barrera, et al., Cancer Treat. Rev. 93 (2021) 102152.
[5] A. Giannis, P. Heretsch, V. Sarli, A. Stößel, Angew. Chem. Int. Ed. 48 (2009) 7911–7914.
[6] H. Shao, W. Liu, M. Liu, et al., J. Am. Chem. Soc. 145 (2023) 25086–25092.
[7] M. Sofiadis, D. Xu, A.J. Rodriguez, et al., J. Am. Chem. Soc. 145 (2023) 21760–21765.
[8] W. Hou, H. Lin, Y. Wu, et al., Nat. Commun. 15 (2024) 5332.
[9] M.M. Logan, T. Toma, R. Thomas-Tran, J. Du Bois, Science 354 (2016) 865–869.
[10] Y. Guo, Z. Guo, J.T. Lu, et al., J. Am. Chem. Soc. 142 (2020) 3675–3679.
[11] Y. Watanabe, H. Morozumi, H. Mutoh, K. Hagiwara, M. Inoue, Angew. Chem. Int. Ed. 62 (2023) e202309688.
[12] Z. Wang, Org. Chem. Front. 11 (2024) 4014–4023.
[13] N.D. Volkow, F.S. Collins, N. Engl. J. Med. 377 (2017) 1797–1798.
[14] K.H. Muchhala, J.C. Jacob, M. Kang, W.L. Dewey, H.I. Akbarali, Physiology 36 (2021) 315–323.
[15] T.Z. Xie, L. Luo, Y.L. Zhao, et al., Org. Lett. 24 (2021) 467–471.
[16] J.J. Wu, Y. Shi, W.S. Tian, Tetrahedron Lett. 56 (2015) 1215–1217.
[17] J.J. Wu, R. Gao, Y. Shi, W.S. Tian, Tetrahedron Lett. 56 (2015) 6639–6642.
[18] X. Li, Y. Zhang, Z. Zhang, J. Wu, Org. Chem. Front. 11 (2024) 3939–3945.
[19] X. Li, Z. Zhang, J. Wu, Angew. Chem. Int. Ed. 64 (2025) e202500341.
[20] L.C. Zhu, D.L. Yang, Y. Shi, Org. Lett. 24 (2022) 5825–5828.
[21] D. Ma, P. Duran, R. Al-Ahmad, et al., J. Am. Chem. Soc. 146 (2024) 16698–16705.
[22] V.A. Schmidt, R.K. Quinn, A.T. Brusoe, E.J. Alexanian, J. Am. Chem. Soc. 136 (2014) 14389–14392.
[23] W.L. Czaplyski, C.G. Na, E.J. Alexanian, J. Am. Chem. Soc. 138 (2016) 13854–13857.
[24] R.K. Quinn, Z.A. Könst, S.E. Michalak, et al., J. Am. Chem. Soc. 138 (2016) 696–702.
[25] C.M. Plummer, H. Zhou, W. Zhu, et al., Polym. Chem. 9 (2018) 1309–1317.
[26] A. Fawcett, M.J. Keller, Z. Herrera, J.F. Hartwig, Angew. Chem. Int. Ed. 60 (2021) 8276–8283.
[27] T.J. Fazekas, J.W. Alty, E.K. Neidhart, et al., Science 375 (2022) 545–550.
[28] A.S. Miller, E.J. Alexanian, Chem. Sci. 13 (2022) 11878–11882.
[29] H. Cao, Y. Kuang, X. Shi, et al., Nat. Commun. 11 (2020) 1956.
[30] H.J. Ringold, S.K. Malhotra, Tetrahedron Lett. 3 (1962) 669–672.
[31] J.A. Edwards, M.C. Calzada, L.C. Ibañéz, A. Bowers, Steroids 6 (1965) 371–396.
[32] R.S.J. Proctor, R.J. Phipps, Angew. Chem. Int. Ed. 58 (2019) 13666–13699.
[33] N. Rodríguez, L.J. Goossen, Chem. Soc. Rev. 40 (2011) 5030–5048.
[34] P.D. Bacoş, A.S.K. Lahdenperä, R.J. Phipps, Acc. Chem. Res. 56 (2023) 2037–2049.
[35] X. Sun, J. Chen, T. Ritter, Nat. Chem. 10 (2018) 1229–1233.
[36] V.T. Nguyen, V.D. Nguyen, G.C. Haug, et al., ACS Catal. 9 (2019) 9485–9498.
[37] J.W. Huffman, R.R. Sobti, Steroids 16 (1970) 755–770.
[38] R.A. Garza-Sanchez, A. Tlahuext-Aca, G. Tavakoli, F. Glorius, ACS Catal. 7 (2017) 4057–4061.
[39] X.L. Lai, X.M. Shu, J. Song, H.C. Xu, Angew. Chem. Int. Ed. 59 (2020) 10626–10632.
[40] L. Tan, H. Kang, M. Liu, et al., Precis. Chem. 1 (2023) 437–442.
[41] K.C. Nicolaou, Y.L. Zhong, P.S. Baran, J. Am. Chem. Soc. 122 (2000) 7596–7597.
[42] Z.H. Shang, Y. Hu, J. Wu, ChemRxiv (2024), doi:10.26434/chemrxiv-2024-pr2tr.